



SciVerse ScienceDirect

J. Mater. Sci. Technol., 2013, 29(7), 619-627



Comparative *in vitro* Study on Pure Metals (Fe, Mn, Mg, Zn and W) as Biodegradable Metals

- J. Cheng¹⁾, B. Liu²⁾, Y.H. Wu¹⁾, Y.F. Zheng^{1,2)*}
- 1) Center for Biomedical Materials and Tissue Engineering, Academy for Advanced Interdisciplinary Studies, Peking University, Beijing 100871, China
- State Key Laboratory for Turbulence and Complex System and Department of Materials Science and Engineering, College of Engineering, Peking University, Beijing 100871, China

[Manuscript received December 13, 2012, in revised form January 30, 2013, Available online 21 March 2013]

Five pure metals including Fe, Mn, Mg, Zn and W have been investigated on their corrosion behavior and *in vitro* biocompatibility by electrochemical measurement, static immersion test, contact angle measurement, cytotoxicity and hemocompatibility tests. It is found that the sequence of corrosion rate of five metals in Hank's solution from high to low is: Mg > Fe > Zn > Mn > W. Fe, Mg and Mg show no cytotoxicity to L929 and ECV304 cells, Mn induces significant cytotoxicity to both L929 and ECV304 cells, and Mg and Mg has almost no inhibition effect on the metabolic activities of ECV304 while largely reduces the cell viability of L929 cells. The hemolysis percentage of five pure metals is lower than 5% except for Mg and platelets adhered on Mg has been activated and pseudopodia-like structures can be observed while platelets on the other four metals keep normal.

KEY WORDS: Biodegradable metals; Cytotoxicity; Corrosion; Biocompatibility

1. Introduction

Biodegradable metallic materials have been considered as a promising candidate for a series of biomedical applications associated with bone^[1] and blood vessels^[2]. Fe-based^[3-5] and Mg-based^[6-8] alloys are two classes of metallic materials that have been widely investigated. In spite of their excellent mechanical properties and biocompatibility, the degradation rate of both pure magnesium and iron can hardly meet the requirements for clinical biomedical applications. As biodegradable materials, the degradation rate of magnesium should be slowed down but for Fe it should be accelerated. That is to say, the ideal degradation rate for biodegradable metals should lie between pure Mg and Fe.

From the viewpoint of corrosion, the standard electrode potential has a substantial effect on the corrosion rate of pure metals. According to the standard electrode potentials of common metals^[9], metals of which standard potential lies between iron and magnesium including Ga, Ta, Cr, Zn, Nb, V, Mn, Zr, Ti, Al, and Be. Among these elements, (1) some elements are

unsuitable for biomedical application due to their toxicity to human body such as Ga, V, Al, Cr and Be^[10–12], (2) pure metals including Ta, Nb, Ti, and Zr are known as valve metals^[13-15] to form a thin oxidation layer on their surface, which greatly enhances the corrosion resistance of the metals^[16,17], so they are considered to be bioinert materials; (3) Zn and Mn have been widely explored as alloying elements in Mg-based^[18,19] and Febased^[20] alloys for biomedical applications. Based on the above consideration, pure metals Zn and Mn are chosen to investigate their potential application as biodegradable metals for bone- or vascular-related applications compared with pure Fe, Mg and W in the present study. We hope to achieve some guidelines for the future design of biodegradable metallic implants. Comprehensive evaluations on the in vitro corrosion behaviors, cytotoxicity as well as hemocompatibility of the five pure metals were conducted.

2. Materials and Methods

2.1. Material preparation

Industrial pure iron with purity of 99.95%, commercially pure Mn with purity of 99.7%, Mg of 99.9%, Zn of 99.99% and W of 99.95% (Cuibolin, Beijing, China) were used as the starting materials. All the five pure metal samples were cut into $10~\text{mm} \times 10~\text{mm} \times 1.5~\text{mm}$ plates for all the tests. Each

^{*} Corresponding author. Prof., Ph.D.; Tel./Fax: +86 10 62767411; E-mail address: yfzheng@pku.edu.cn (Y. F. Zheng).

^{1005-0302/\$ –} see front matter Copyright © 2013, The editorial office of Journal of Materials Science & Technology. Published by Elsevier Limited. All rights reserved.

specimen was mechanically polished up to 2000 grit, and then ultrasonically cleaned in absolute ethanol. For cytotoxicity tests, specimens were further sterilized by ultraviolet-radiation for at least 2 h.

2.2. Electrochemical measurement

A traditional three-electrode cell was used for the electrochemical measurements on an electrochemical workstation (CHI660C, China) in Hank's solution^[21]. A platinum electrode was set as the auxiliary electrode and a saturated calomel electrode (SCE) as the reference electrode, respectively. All the parameters and procedures in the electrochemical measurement were set as same as described in our previous work reported by Liu et al.^[3].

2.3. Static immersion test

The immersion test was performed in Hank's solution according to ASTM-G31-72^[22]. Experimental samples were immersed in 50 ml solution at the temperature of 37 °C. After 3-, 10- and 30-day immersion, the samples were removed from Hank's solution, rinsed with distilled water, and dried in air. The changes on the surface morphology of the specimens after immersion were characterized by environmental scanning electron microscopy (ESEM, AMRAY-1910FE). Inductively coupled plasma-atomic emission spectroscopy (ICP-AES) (Leeman, Profile) was explored to determine the ion concentrations released into Hank's solution after the corrosion products were completely dissolved by HNO3. X-ray photoemission spectroscopy (XPS) analysis was performed to analyze the surface composition of specimens after they were immersed in Hank' solutions for 3 days with an Axis Ultra spectrometer using mono AlK α (1486.6 eV) radiation at vacuum pressure of 10^{-9} bar (10⁻⁴ Pa), 15 kV, and 15 mA. The binding energy was calibrated by using Cls hydrocarbon peak at 284.8 eV.

2.4. Contact angle measurement

The surface wettability was tested by contact angle (Dataphysics Instruments, Germany) in triple for each sample and two samples were used for each pure metal. Briefly, a 2 μ L droplet of pure water was suspended from the tip of the microliter syringe supported above the sample stage. The image of the droplet was captured and the contact angle was measured by using the OCA20 drop shape analysis program (Dataphysics Instruments, Germany).

2.5. Cytotoxicity test

Murine fibroblast cells (L929) and human umbilical vein endothelial cells (ECV304) were adopted to evaluate the cytotoxicity of five pure metals according to ISO 10993-12^[23] by indirect contact assay. Both L929 and ECV304 cells were cultured in the Dulbecco's modified Eagle's medium (DMEM) supplemented with 10% fetal bovine serum (FBS), 100 U/ml penicillin and 100 μg/ml streptomycin at 37 °C in a humidified atmosphere of 5% CO₂. The specimens were incubated in DMEM serum free medium for 72 h with the surface area/extraction medium ratio of 1.25 cm²/ml in a humidified atmosphere with 5% CO₂ at 37 °C. After that, the supernatant fluid was withdrawn and centrifuged to prepare the extraction

medium, then stored at 4 °C before the cytotoxicity test. In the control groups, DMEM medium was used as negative control and 10% DMSO (dimethly sulfoxide) DMEM medium as positive control. Cells were seeded in 96-well cell culture plates at 5×10^3 cells/100 µL medium in each well and incubated for 24 h. The medium was then replaced with 100 μL of prepared extraction medium. After incubating the cells in the incubator for 1, 2 and 4 days, respectively, an optical microscope was used to observe the morphologies of cells. Then, 10 µL MTT (3-(4, 5dimethylthiazol-2-yl)-2, 5-diphenyltetrazolium bromide) was added to each well and the specimens were incubated with MTT for 4 h in the incubator. Thereafter, 100 µL formazan solubilization solution (10% SDS (sodium dodecyl sulfate) in 0.01 mol/ L HCl) was added to each well and incubated overnight in the incubator. The optical density of the solutions was measured by microplate reader (Bio-RAD680) at 570 nm with a reference wavelength of 630 nm. The concentrations of released pure metal ions in the extracts were also measured by ICP-AES.

2.6. Hemolysis test

Health human blood from a volunteer was mixed with sodium citrate (3.8 wt%) in the ratio of 9:1 and diluted with physiological saline at a volume ratio of 4:5. Pure metals specimens were dipped in centrifuge tubes containing 10 ml of physiological saline and they were incubated at 37 °C for 30 min. Then 0.2 ml of diluted blood was added to these tubes, respectively and the mixtures were incubated at 37 °C for 60 min. Normal saline solution was used as a negative control and deionized water as a positive control. Thereafter, specimens were removed and all the tubes were centrifuged at 800 g for 5 min. The supernatant from each tube was transferred to a cuvette where the absorbance was measured by microplate reader at 545 nm. The hemolysis was calculated as follows:

$$Hemolysis = \frac{OD(\text{test}) - OD(\text{negative} \text{control})}{OD(\text{positive} \text{control}) - OD(\text{negative} \text{control})} \times 100\%$$

where OD = optical density at 545 nm.

2.7. Platelet adhesion

Platelet-rich plasma (PRP) was prepared by centrifuging the whole human blood from a volunteer at 200 g for 15 min. The experimental specimens were covered by PRP and incubated at 37 °C for 1 h. After that the specimens were gently rinsed with phosphate buffer saline (PBS). They were then fixed in 2.5% glutaraldehyde solutions for 1 h at room temperature followed by dehydration in a gradient ethanol/distilled water mixture from 50% to 100% in 10% increments for 10 min each and finally dried for 2 days. The surfaces of platelet-attached plates were observed by ESEM.

3. Results

3.1. Corrosion behavior

3.1.1. Electrochemical corrosion behavior. The corrosion potential values as a function of immersion time for Fe, Mn, Mg, Zn and W in Hank's solution were investigated in the open circuit potential (OCP), as shown in Fig. 1(a). A continuously

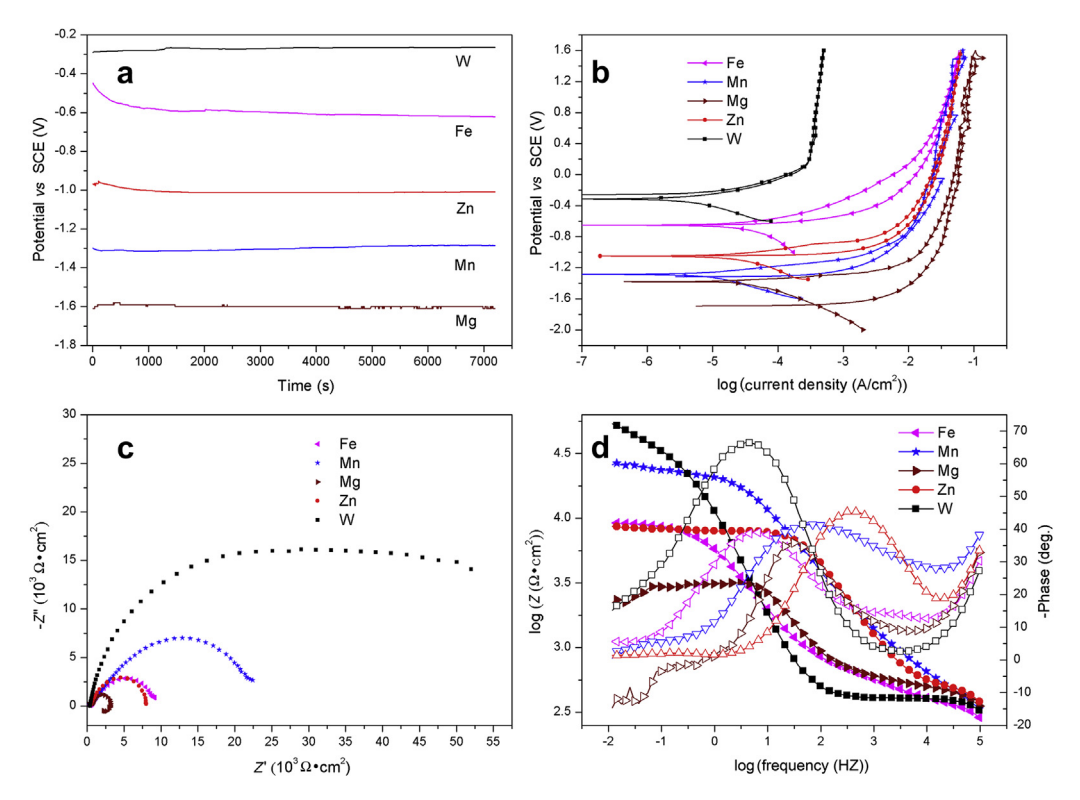


Fig. 1 Electrochemical corrosion results of pure metals (Fe, Mn, Mg, Zn and W) in Hank's solutions: (a) OCP curves; (b) potentiodynamic curves; (c) Nyquist diagram; (d) Bode diagram.

reduced potential process of Fe in Hank's solution can be found in the beginning of the test. It indicates that the potential of corrosion products is lower than that of pure metal for Fe. For these five pure metals, the sequence of OCP from high to low is: W>Fe>Zn>Mn>Mg. Mg is the most active metal among these pure metals, and the OCP curve of Mg is more unstable than the other four curves.

Fig. 1(b) presents the potentiodynamic polarization curves of Fe, Mn, Mg, Zn and W specimens immersed in Hank's solution. The average electrochemical parameters and corrosion rate are listed in Table 1. It can be seen that the sequence of corrosion potential in Hank's solution from high to low is: W > Fe > Zn > Mn > Mg. The standard electrode potential of W, Fe, Zn, Mn, Mg is -0.05, -0.44, -0.76, -1.18 and -2.37 V (vs SCE), respectively. Therefore, the sequence of corrosion potential in Hank's solution corresponded to that of the standard electrode potential for these five pure metals. Except for Mg, corrosion potential in Hank's solution is lower than the standard electrode potential for all these metals because of the high concentration of Cl^- ion in Hank's solution.

Table 1 Electrochemical data and corrosion rate of Fe, Mn, Mg, Zn and W in Hank's solutions

	V _{corr} (V)	I _{corr} (A/cm ²)	V _{corr} (mm/year)
W	-0.313	0.97	0.030
Zn	-1.049	5.47	0.325
Mn	-1.285	2.06	0.102
Fe	-0.748	8.96	0.105
Mg	-1.886	86.06	1.94

Notes: $V_{\rm corr} =$ corrosion potential, $I_{\rm corr} =$ corrosion current densities, $V_{\rm corr} =$ corrosion rate in terms of penetration rate.

The sequence of corrosion current densities in Hank's solution from high to low is: Mg > Fe > Zn > Mn > W. Generally, lower corrosion potential implies higher corrosion current densities. However, the electrochemical data of Fe, Zn and Mn in the tests are against the common rule and the corrosion current densities of these three pure metals are close and in the same order of magnitude.

The forward polarization curve of W is almost coincided with the reverse polarization curve. It indicates that the surface of W does not significantly change even in +1.6 V voltage. After polarization test, there are no corrosion pits on the surface of W.

The results of the electrochemical impedance spectroscopy (EIS) measurements in simulated body fluid (SBF) are shown in Fig. 1(c) and (d) as Nyquist plots and Bode plots. The sequence of polarization resistance in Hank's solution from high to low is: $Mg > Fe \approx Zn > Mn > W$. It is similar to the sequence of corrosion current densities.

3.1.2. Immersion corrosion behavior. Fig. 2 reveals the released ion concentrations of Fe, Mn, Mg, Zn and W in Hank's solution at different immersion intervals. The corresponding surface morphologies after immersed in Hank's solution for 30 days are shown in Fig. 3. It can be seen that the sequence of released ion concentrations of five pure metals in the first 10-day immersion from high to low is: $Mg > W > Mn > Fe \approx Zn$. The concentrations of released Fe and Zn ions are much lower than those of the other three kinds of metal ions. According to the results of electrochemical measurement results, the corrosion rates of Fe and Zn are faster than that of W. The reason is that most corrosion products of Fe and Zn are insoluble and the insoluble corrosion products are not dissolved by HNO₃ before the ICP—AES test.

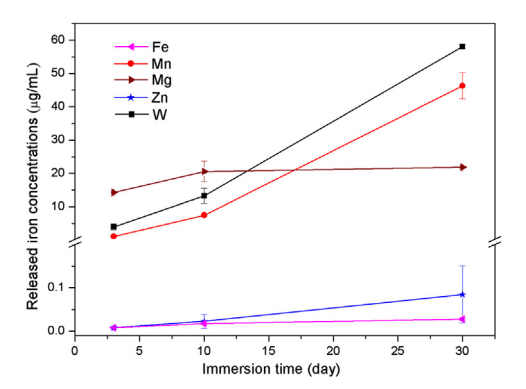


Fig. 2 Released ion concentrations of pure metals (Fe, Mn, Mg, Zn and W) in Hank's solution for 3, 10 and 30 days.

The insolubility of Fe(OH)₃ and Zn(OH)₂ leads to the low ion concentrations in Hank's solution.

On the other hand, the sequence of released ion concentration of five pure metals after 30-day immersion in Hank's solution from high to low is: W>Mn>Mg>Fe>Zn. The concentration of Mg ion has reached saturation after 10 days since the corrosion product $Mg(OH)_2$ is micro-soluble in water. Consequently, even if the corrosion rate of Mg is the fastest among these five pure metals, the concentration of Mg ion in Hank's solution is only 20 μ g/ml after 30-day immersion and it is lower than the concentration of W and Mn.

Corrosion products of Fe and Zn are insoluble. As a result, the corrosion products of Fe and Zn significantly increase after 30-day immersion but the released ion concentration in Hank's solution does not change too much. Therefore, even though the corrosion rates of Fe-based and Zn-based alloys will be much faster in the future, the complete degradation of these alloys are

hard to come true if there are no effective mechanisms to transport the insoluble corrosion products out of the body.

After 30-day immersion, the surface morphology of W specimen is similar to the original state in the large scale and it shows a typical phenomenon of general corrosion. However, the surface becomes rougher in the small scale. The corrosion type of Zn and Fe is localized corrosion. The corrosion products bunch together, while the part of the specimen where corrosion does not occur remains bright metallic luster. Mg specimens are totally degraded after 30-day immersion so the surface morphology cannot be obtained.

The XPS spectra of pure metals (Fe, Mn, Mg, Zn and W) after 3day immersion in Hank's solution are shown in Fig. 4. Fe2p peak locates at binding energy of Fe2p3/2 711.4 eV and Fe2p1/2 724.6 eV. It indicates the existence of Fe₂O₃ and the chemical valence of Fe in corrosion products is +3. Mn2p mixed peaks denote to MnO (Mn2p3/2 641.3 eV and corresponding shake-up peak 646.3 eV), MnO₂ (Mn2p3/2 642.5 eV) and Mn₂O₃ (Mn2p1/ 2 653.4 eV and corresponding shake-up peak 658.4 eV). It suggests the chemical valence of Mn in corrosion products is +2 and +4, respectively. Mg2p peak located at 50.2 eV is assigned to the appearance of MgO. Zn2p peak located at Zn2p3/2 1022.5 eV indicates that the chemical valence of Zn in corrosion products is +2. W4f peaks are composed of WO₃ (W4f5/2 37.7 eV and W4f7/2 35.6 eV), WC (W4f5/2 32.2 eV) and W (W4f5/2 33.4 eV and W4f7/ 2 31.1 eV). It indicates the existence of WO₃ and WC in the corrosion products. Because of the slow corrosion rate of W, the peak of simple substance W can be found after 3 days immersion.

3.2. Contact angle test

Fig. 5 shows the contact angles of five pure metals (Fe, Mn, Mg, Zn and W). The sequence of contact angle for the five pure metals from high to low is: Mn > Mg > Fe > Zn > W, revealing

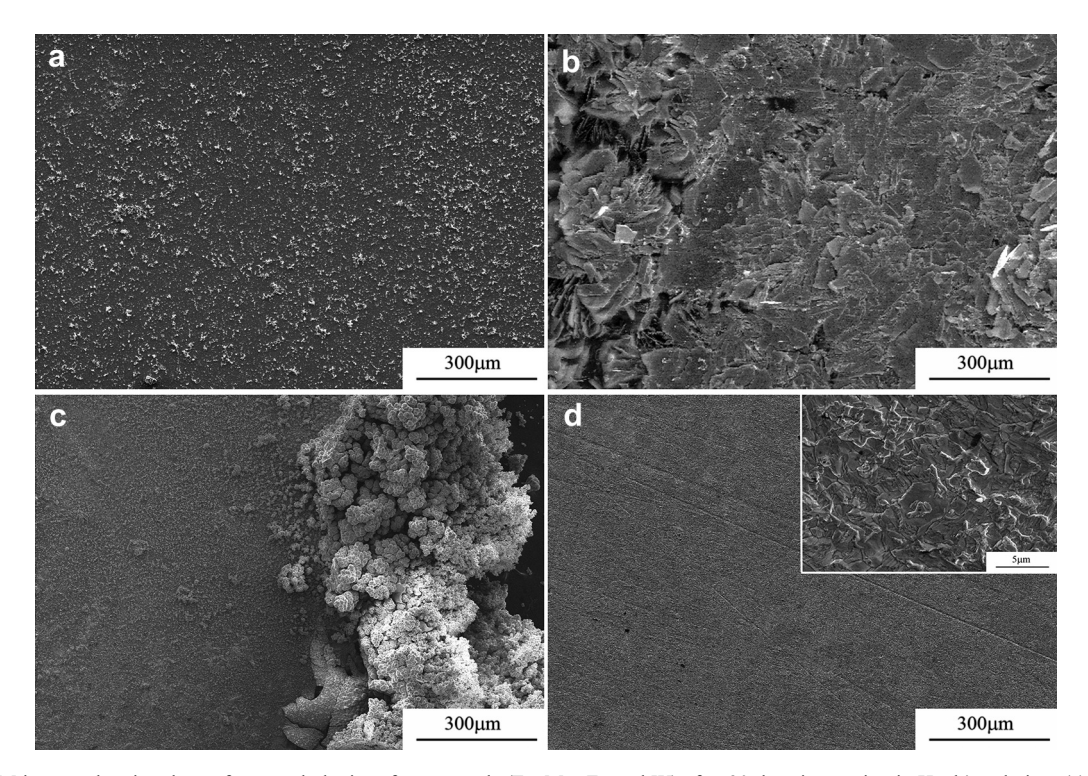


Fig. 3 SEM images showing the surface mophologies of pure metals (Fe, Mn, Zn and W) after 30 days immersion in Hank's solution: (a) Fe, (b) Mn, (c) Zn, (d) W. Mg specimen was totally degaraded after 30 days immersion.

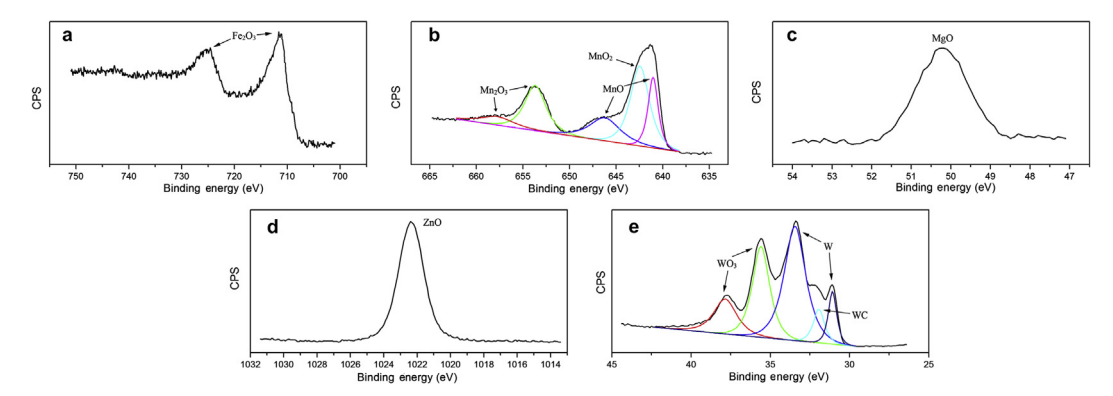


Fig. 4 XPS spectra of pure metals (Fe, Mn, Mg, Zn and W) after 3 days immersion in Hank's solution: (a) Fe2p, (b) Mn2p, (c) Mg2p, (d) Zn2p, (e) W4f.

that W has the best hydrophilicity while Mn is the worst among the five pure metals. Generally, the smaller the contact angle and the higher the surface energy, the stronger the hydrophilicity of materials, and also the more conducive it is to cell adhesion. It is well known that high hydrophilicity has an important significance for cardiovascular stents and contributes to cell adhesion on the surface of materials^[24].

3.3. Cytotoxicity evaluation

Fig. 6(a) and (b) illustrates the cell viability of murine fibroblast cells L929 and human umbilical vein endothelial cells ECV304, respectively, expressed as a percentage of the viability of cells cultured in the negative control after 1, 2, and 4 days incubation in the extraction medium of five pure metals. It can be seen that the L929 cell viabilities decrease as the incubation time increases after being incubated in the extracts of Mn and Zn, and significant cytotoxicity can be found for them. However, no reduced cell viabilities in extracts of Mg and W, while a little less than 90% cell viability in extracts of Fe can be observed. For ECV304 cells, Mn shows strong cytotoxicity and Fe, Zn, W have slight cytotoxicity with about 90% cell viability after 4 days incubation in the extracts of them, whereas Mg almost shows no reduced cell viability. Fig. 6(c) describes the released ion concentration of pure metals in the extraction medium. The

sequence of ion concentration of five pure metals from high to low is $Mg > W > Fe > Zn \approx Mn$.

Fig. 7 shows the morphologies of L929 cells cultured in the extraction medium for 4 days. Cells in the extracts of Fe, Mg and W exhibit healthy morphologies with flattened spindle shapes, but cells in the extracts of Mn and Zn have almost died with only a few amounts of normal cells compared with the negative control. The results are basically consistent with those of cell viabilities discussed in Fig. 6(a).

3.4. Hemocompatibility evaluation

Fig. 8 shows the hemolysis percentage of experimental pure metals. The hemolysis ratios of Fe, Mn, Zn and W are less than 3%, much lower than 5%, a judging criterion for excellent blood compatibility^[25], whereas the hemolysis percentage of pure Mg reaches 37%, which is much larger than 5%. This might be ascribed to the high corrosion rate of pure Mg and large pH variation after 1 h incubation in saline solution^[26].

The morphologies of adhered human platelet on the pure metal specimens are shown in Fig. 9. It can be seen that platelets keep the shape of round on the surfaces of Mn, Mg and W, without any sign of pseudopodia-like structures. Most of platelets on the surface of Fe keep round shape, with one or two pseudopodia spreading out. Platelets on the surface of Zn have

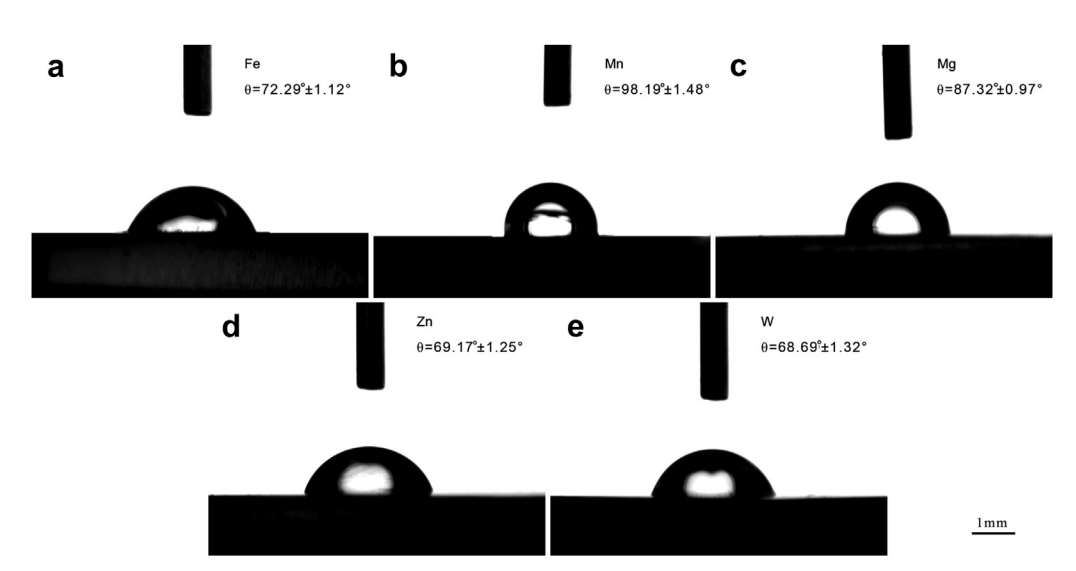


Fig. 5 Optical images showing the contact angle of pure metals: (a) Fe, (b) Mn, (c) Mg, (d) Zn and (e) W.

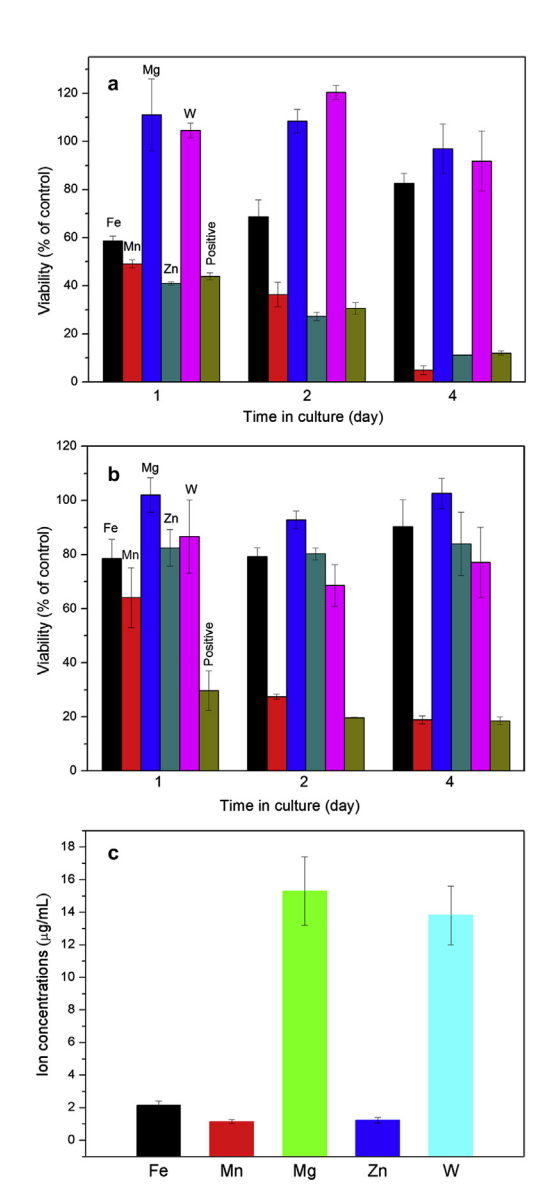


Fig. 6 Cell viability of (a) L929, (b) ECV304 after 1, 2 and 4 days incubation in pure metals (Fe, Mn, Mg, Zn and W) extraction mediums; (c) released ion concentrations in extraction mediums used for cytotoxicity tests.

all been activated and spread out. The amount of adhered platelets on the surfaces of Mn, Zn and W are much larger than that on Fe and Mg. Besides, corrosion products can be found on the surfaces of Mg and Zn, while Ca/P compounds are observed to precipitate on the surface of Fe.

4. Discussion

In the present study, the *in vitro* corrosion behavior and biocompatibility of five pure metals including Fe, Mn, Mg, Zn as well as W were investigated.

4.1. Comparison on mechanical properties of Fe, Mn, Mg, Zn and W

The properties of pure metals, such as mechanical properties, melting point play a significant role in the consideration for materials preparation and applications. Table 2 summarizes the general properties of these five pure metals and typical new alloy systems reported. For pure Mn, it has a relatively low yield strength (YS) and ultimate strength (US), which cannot provide sufficient mechanical support. The YS and US of W are relatively high with an elastic modulus much higher than that of human bone and vessel wall. For pure Zn, its US is a little higher than that of Mg, however, it is a brittle material with a brittle fracture mode. Thus, Zn may be suitable for bone fixation but improper for stent applications, in which good ductility is needed. Pure Mg has a density and elastic modulus close to that of human bone with slightly low YS and US. Alloying is needed to improve the mechanical properties of Mg-based materials for both bone and vascular stent applications. Pure Fe possesses the most suitable mechanical properties among these five pure metals for coronary stent material as it is most likely to replicate the mechanical properties of 316L SS.

On the other hand, a single pure metal can hardly meet all the requirements for biomedical applications. In most cases, alloying elements must be added to form alloys in order to improve their mechanical properties. Zn and Mg belong to metals with low-melting-point while the melting point of Fe and Mn are high and W has the highest melting point. Generally, it is difficult to fabricate alloys by traditional casting technology when there is a big difference between the melting points of two alloying elements. In addition, elements with high melting point can be added into a low-melting-point metal to form alloys by chemical reaction. Therefore, Zn and Mn are suitable alloying elements for Mg while Mn, W are suitable for Fe. Actually, in literature Mg–Zn–(Mn, Ca)^[18,27,28] and Fe–Mn^[20,29], Fe–Mn–Pd^[5], Fe–Wn–Pd^[5], Fe–Wn^[3] alloys have been reported as biodegradable biomaterials with superior mechanical properties and degradation behaviors.

4.2. Comparison on degradation rate of Fe, Mn, Mg, Zn and W

Fe-based and Mg-based alloys are two typical classes of materials used for biodegradable implants. For coronary stent application, previous research results have indicated that the degradation rate of Mg-based alloys should be slowed down, while for pure iron an elevated degradation rate is desired^[5]. As for W, no results have been reported on using pure W as biodegradable metal, however, early animal test has confirmed the degradation of W in vivo $^{[30]}$, despite the fact that the degradation rate of W is extremely low^[31]. Pure Zn and Mn have not been reported for biomedical applications, but they have been used as controls in the research of Zn-based alloys [32] and Fe-Mn alloys^[20], respectively. The sequence of degradation rate of pure metals in Hank's solution from high to low in the present study is: Mg > Fe > Zn > Mn > W. Theoretically, the proper degradation rate of material for coronary stent should lie between pure Mg and Fe^[4]. Thus, pure Zn, Mn and W are improper as biodegradable stent implants due to their low degradation rate in physiological environment, even though the corrosion mode of W turns out to be uniform corrosion and its corrosion products are soluble, which matches well with the requirements for biodegradable stents. On the other hand, in the case of bone fixation, Fe-based alloys have been studied considering their superior mechanical properties and relatively low corrosion rate compared with Mg alloys^[33]. Znbased Zn-Mg alloys have also been reported for bone fixation because of their high corrosion resistance and low hydrogen evolution rate in comparison to Mg alloys^[32]. However, much in vivo trails have to be done to validate their biocompatibility, biofunctionality and biodegradability before Fe-based and Zn-based alloys being developed as bone-related implants.

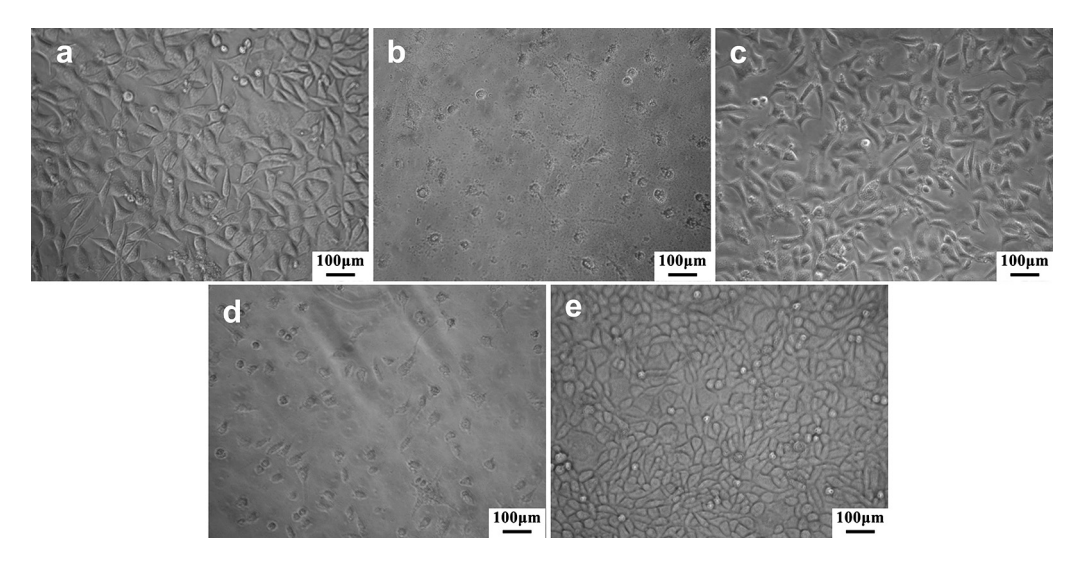


Fig. 7 Optical images of L929 cells that cultured in (a) Fe, (b) Mn, (c) Mg, (d) Zn and (e) W extraction mediums for 4 days.

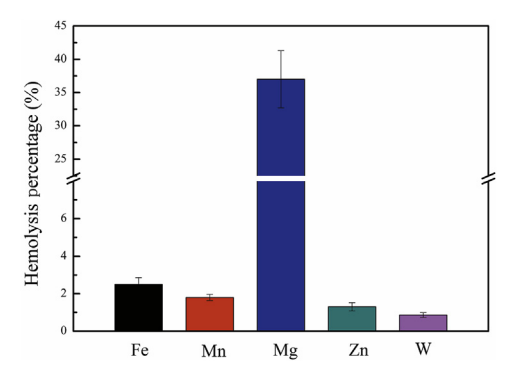


Fig. 8 Hemolysis percentage of pure metals (Fe, Mn, Mg, Zn and W).

4.3. Comparison on biocompatibility of Fe, Mn, Mg, Zn and W

4.3.1. Cytotoxicity. Fe^[34] and Mg^[1] are essential elements for human body with significant functional role in biological systems. Preliminary *in vivo* animal test results have demonstrated

their good biocompatibility that there is no occurrence of acute neointimal proliferation and no local or systemic toxicity after the implantation of pure iron stents^[35,36] and WE43 Mg alloy stents^[37,38]. For W, it is a kind of material that has been widely used as coils for the occlusion of arterial aneurysms and the degradation of W is not associated with local or systemic toxicity^[30]. The *in vitro* cytotoxicity results in the present work indicate that pure Fe, Mg and W do not present any cytotoxic effects on L929 and ECV304 cells and exhibit excellent biocompatibility, which is in good consistence with results reported in other literature^[3,7,31], though the ion concentrations of Mg and W in the extract medium are higher than those of other three metals. For Mn, significantly reduced cell viability of both L929 and ECV304 cells is observed after incubation in the extracts of pure Mn, indicating obvious cytotoxicity. Hermawan et al. [20] also reported that Mn powders show significant inhibitory effect on the metabolic activities of 3T3 fibroblast cells. However, when Mn acts as an alloying element, the metabolic inhibition is greatly lowered in Fe-Mn^[20] and Mg-

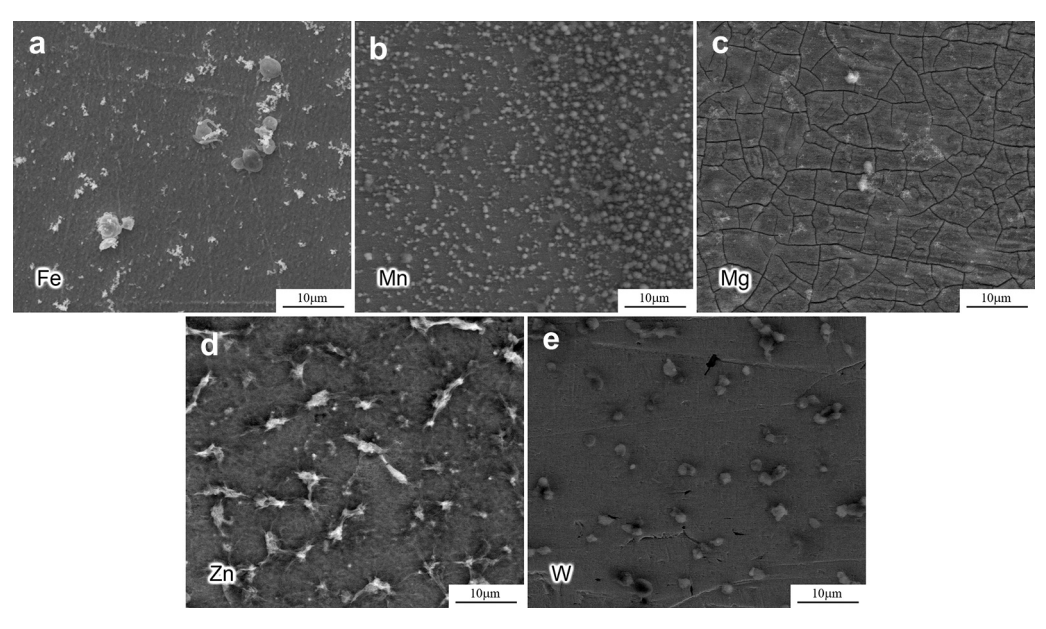


Fig. 9 SEM images of platelets adhering to pure metals: (a) Fe, (b) Mn, (c) Mg, (d) Zn and (e) W.

	ρ (g/cm ³)	Melting point, $T_{\rm m}$ (°C)	Elastic modulus (GPa)	Yield strength (MPa)	Ultimate strength (MPa)	Cytotoxicity grade	New alloy systems reported
Fe	7.87	1538	211	120-150	180-210	1 to L929 and ECV304	Fe-Mn ^[20] , Fe-W ^[3] , Fe-Mn-Pd ^[5] , Fe-Mn-Si ^[39]
Mn	7.21	1246	_	<5	<5	4 to L929 and ECV304	Alloying elements for Fe ^[20] , Mg ^[27]
Mg	1.74	660	45	80	152	0-1 to L929 and ECV304	Mg-Ca ^[40] , Mg-Zn ^[18] , Mg-Mn ^[41] , Mg-Zn-Mn ^[27] , Mg-Zn-Ca ^[28]
Zn	7.14	419.5	105	_	110-200	4 to L929 and 1 to ECV304	Zn-Mg ^[32] , to be explored
W	19.25	3422	411	550	550-620	0-1 to L929 and ECV304	Alloying element for Fe

Table 2 General properties of five pure metals and new alloy systems of five metals reported

Mn–Zn^[19] alloys, even when the amount of Mn comes up to 35 wt% in Fe. Pure Zn exhibits no obvious cytotoxicity to ECV304 cells but significantly reduces the cell viability of L929 cells, indicating that Zn may be suitable for vascular-related applications. Further researches on the cytotoxicity of Zn-based alloys are needed.

4.3.2. Hemocompatibility. It is noted that pure Mg leads to high hemolysis ratio and the result is in good consistence with previous reported results, which may be ascribed to the fast corrosion rate of Mg^[7]. Measures such as alloying should be taken to enhance the corrosion resistance of Mg before it can be used for stent applications. For the other four pure metals, the hemolysis percentage are all less than 5% and platelets adhered on the surface of these metals keep normal round shape except for Zn, indicating good hemocompatibility of pure Fe, Mn and W. However, considering that the hemolysis ratio of Mg alloys decreases with the enhancement of corrosion resistance, attention on the thrombogenicity of these pure metals still should be paid when efforts such as alloying and surface modification are taken to obtain accelerated corrosion rate.

In conclusion, all these five pure metals can hardly satisfy the demands for biomedical applications. From the viewpoint of alloying, it is promising to develop Fe-based, Mg-based alloys so as to obtain superior mechanical properties and moderate corrosion rate. Mn is an ideal alloying element for both Fe and Mg. Zn is a suitable alloying element for Mg-based alloys with excellent strength as well as high corrosion resistance^[7]. As for Zn-based alloys, more works can be explored as biodegradable implant materials.

5. Conclusions

- Fe exhibits excellent biocompatibility (cytotoxicity and hemocompatibility) and relatively low corrosion rate in Hank's solution. Mn and W would be suitable alloying elements for Fe.
- (2) Mn shows significant cytotoxicity to both L929 and ECV304 cells, indicating that it is improper for biomedical applications but may be ideal alloying element for both Fe and Mg with moderate amount.
- (3) Mg exhibits no cytotoxicity to L929 and ECV304 cells but leads to high hemolysis ratio. Mn and Zn may be suitable alloying elements to enhance its corrosion resistance.
- (4) Zn shows no cytotoxicity to ECV304 cells while significantly reduces cell viability of L929 cells. It is still to be explored for Zn-based alloys as biodegradable metals.
- (5) W is unsuitable for biodegradable material because of its low corrosion rate in physiological environment, though it exhibits excellent biocompatibility.

Acknowledgments

This work was supported by the National Basic Research Program of China (973 Program) (Nos. 2012CB619102 and 2012CB619100), the Research Fund for the Doctoral Program of Higher Education (No. 20100001110011), the National Science Fund for Distinguished Young Scholars (No. 51225101), the National Natural Science Foundation of China (No. 31170909) and the Guangdong Innovative Research Team Program (No. 201001C0104669453).

REFERENCES

- M.P. Staiger, A.M. Pietak, J. Huadmai, G. Dias, Biomaterials 27 (2006) 1728–1734.
- [2] R. Waksman, J. Interv. Card. 19 (2006) 414-421.
- [3] B. Liu, Y.F. Zheng, Acta Biomater. 7 (2011) 1407-1420.
- [4] H. Hermawan, D. Dubé, D. Mantovani, Acta Biomater. 6 (2010) 1693–1697.
- [5] M. Schinhammer, A.C. Hänzi, J.F. Löffler, P.J. Uggowitzer, Acta Biomater. 6 (2010) 1705—1713.
- [6] F. Witte, J. Fischer, J. Nellesen, H.A. Crostack, V. Kaese, A. Pisch, F. Beckmann, H. Windhagen, Biomaterials 27 (2006) 1013–1018.
- [7] X. Gu, Y. Zheng, Y. Cheng, S. Zhong, T. Xi, Biomaterials 30 (2009) 484–498.
- [8] G. Song, S. Song, Adv. Eng. Mater. 9 (2007) 298-302.
- [9] G. Milazzo, S. Caroli, R.D. Braun, J. Electrochem. Soc. 125 (1978) 260C–261C.
- [10] J.L. Yang, H.C. Chen, Chemosphere 53 (2003) 877-882.
- [11] S.S.A. El-Rahman, Pharm. Res. 47 (2003) 189-194.
- [12] L. Fishbein, Int. J. Environ. Anal. Chem. 17 (1984) 113-170.
- [13] N.T.C. Oliveira, S.R. Biaggio, R.C. Rocha-Filho, N. Bocchi, J. Biomed. Mater. Res. A 74 (2005) 397–407.
- [14] O.E. Linarez Pérez, V.C. Fuertes, M.A. Pérez, M. López Teijelo, Electrochem. Commun. 10 (2008) 433–437.
- [15] A. Davydov, Electrochim. Acta. 46 (2001) 3777-3781.
- [16] S. Zein El Abedin, U. Welz-Biermann, F. Endres, Electrochem. Commun. 7 (2005) 941–946.
- [17] S.K. Cho, I.S. Park, S.J. Lee, K.A. Kim, J.M. Park, S.G. Ahn, K.Y. Song, D.J. Yoon, M.H. Lee, Surf. Interface Anal. 44 (2012) 114—120.
- [18] S. Zhang, X. Zhang, C. Zhao, J. Li, Y. Song, C. Xie, H. Tao, Y. Zhang, Y. He, Y. Jiang, Acta Biomater. 6 (2010) 626—640.
- [19] L. Xu, G. Yu, E. Zhang, F. Pan, K. Yang, J. Biomed. Mater. Res. A 83 (2007) 703-711.
- [20] H. Hermawan, A. Purnama, D. Dube, J. Couet, D. Mantovani, Acta Biomater. 6 (2010) 1852–1860.
- [21] E. Chang, T. Lee, Biomaterials 23 (2002) 2917-2925.
- [22] ASTM-G31-72, Annual Book of ASTM Standards, American Society for Testing and Materials, Philadelphia, Pennsylvania, USA, 2004.
- [23] E. ISO10993-12, German Version: DIN EN ISO (2008) 10993-10912.
- [24] L.F. Zhao, Y. Hong, D.Y. Yang, X.Y. Lv, X.T.F. Xi, D.Y. Zhang, Y. Hong, J.F. Yuan, Biomed. Mater. 6 (2011) 025012.
- [25] ASTM F756-08, Annual Book of ASTM Standards, American Society for Testing and Materials, Philadelphia, Pennsylvania, USA, 2008.

- [26] X. Gu, W. Zheng, Y. Cheng, Y. Zheng, Acta Biomater. 5 (2009) 2790–2799.
- [27] H. Wang, S. Guan, X. Wang, C. Ren, L. Wang, Acta Biomater. 6 (2010) 1743–1748.
- [28] L. Yang, E. Zhang, Mater. Sci. Eng. C 29 (2009) 1691-1696.
- [29] H. Hermawan, D. Dubé, D. Mantovani, J. Biomed. Mater. Res. A 93 (2010) 1–11.
- [30] M. Peuster, C. Fink, P. Wohlsein, M. Bruegmann, A. Günther, V. Kaese, M. Niemeyer, H. Haferkamp, C. Schnakenburg, Biomaterials 24 (2003) 393–399.
- [31] M. Peuster, Biomaterials 24 (2003) 4057-4061.
- [32] D. Vojtěch, J. Kubásek, J. Šerák, P. Novák, Acta Biomater. 7 (2011) 3515–3522.
- [33] B. Wegener, B. Sievers, S. Utzschneider, P. Müller, V. Jansson, S. Rößler, B. Nies, G. Stephani, B. Kieback, P. Quadbeck, Mater. Sci. Eng. B 176 (2011) 1789—1796.

- [34] G. Papanikolaou, K. Pantopoulos, Toxicol. Appl. Pharmacol. 202 (2005) 199–211.
- [35] M. Peuster, P. Wohlsein, M. Brgmann, M. Ehlerding, K. Seidler, C. Fink, H. Brauer, A. Fischer, G. Hausdorf, Heart 86 (2001) 563.
- [36] M. Peuster, C. Hesse, T. Schloo, C. Fink, P. Beerbaum, C. von Schnakenburg, Biomaterials 27 (2006) 4955–4962.
- [37] R. Waksman, R. Pakala, P.K. Kuchulakanti, R. Baffour, D. Hellinga, R. Seabron, F.O. Tio, E. Wittchow, S. Hartwig, C. Harder, Catheter. Cardio. Interv. 68 (2006) 607–617.
- [38] R. Waksman, R. Pakala, T. Okabe, D. Hellinga, R. Chan, M.I.N.O. Tio, E. Wittchow, S. Hartwig, K.H. Waldmann, C. Harder, J. Interv. Cardiol. 20 (2007) 367–372.
- [39] B. Liu, Y.F. Zheng, L. Ruan, Mater. Lett. 65 (2011) 540-543.
- [40] Z. Li, X. Gu, S. Lou, Y. Zheng, Biomaterials 29 (2008) 1329-1344.
- [41] Y. Xin, T. Hu, P.K. Chu, Acta Biomater. 7 (2011) 1452-1459.